北海道大学工学部研究報告
第145号（昭和63年）

Bulletin of the Faculty of Engineering,
Hokkaido University, No. 145 (1988)

(Three-Dimensional R/C Beam-Column Subassemblages with Slabs)

BEHAVIOR OF THREE-DIMENSIONAL REINFORCED CONCRETE BEAM-COLUMN SUBASSEMBLAGES WITH SLABS

Osamu JOH, Yasuaki GOTO and Takuji SHIBATA

(Received September10, 1988)

Abstract

An experimental study was carried out to clarify the shear resistance behavior of interior beam-column joints in two-way reinforced concrete frames. Four three-dimensional subassemblages with slabs are used as specimens to which lateral cyclic forces are applied in two directions perpendicular to each other by changing the direction alternately at every cycle. On the basis of the results of experiment and calculation, effective width of slabs participating in the bending strength of beams, ultimate strength of joint panels, effectiveness of the panel stiffness in story drift and energy absorption are discussed. As for the ultimate strength of joint panels, adaptability of two equations previously proposed in Japan and reasonableness of the requirements of ACI Code and New Zealand Standard also are discussed in comparison with the test results.

1. Introduction

Beam-column joints in space frames are usually subjected to two-way lateral cyclic forces during earthquakes as well as the columns of the frames. However, the shear resistance behavior of the beam-column joints has not been defined in spite of their importance. Although experimental work on the behavior of beam-column joints to subjected one-directional cyclic lateral loading have been carried out by many researchers, only a small number of tests on those subjected to two-directional loading have been reported.

In particular, very few tests of the three dimensional beam column subassemblages with slab have been carried out. In this paper, the shear resistance behavior is discussed by using the test results of four half-scale interior beam-column joint specimens with two-way beams and slabs. The variations in the specimens were made by the lateral loading direction, the lateral reinforcement in joint and the beam-column depth ratio. A one-way frame joint specimen without transverse beams and slabs of the previous test series is compared

Department of Architecture

with the present specimens.

2. Experimental Work

2.1 Description of Specimens

The specimens were assumed to be a part of a space frame subjected to earthquake forces, and being cut off at six inflection points in four beams and two columns adjoining an interior joint. The overall dimensions of the specimens were identical in the four specimens as shown in Fig. 1, and the principal dimensions were identical in the one-way frame joint specimen. The distances from the joint center to the beam-end supports and to the column end loading points were 1500 mm and 875 mm, respectively. The cross-sections of columns were 300 mm x 300 mm in all specimens. The cross-sections of beams were 150 mm x 350 mm in four specimens (X2-1, X2-2, X2-3, and X0-1), and 150 mm x 600 mm in one specimen (X2-4). The thickness of slabs was 60 mm.

All the specimens were designed to develop weak-beam strong-column behavior on the assumption that the participating width of slabs in bending strength of the adjoining beams would be their entire width. The details of specimens are shown in Fig.1. The indexes of the properties of the specimens are summarized in Table 1.

The specimens 'X2-1' and 'X2-2' were wholly identical in detail with each other, of which the only difference was in the loading directions, and were the same as ones which provided the slabs and transverse beams for the specimen 'X0-1'. The joint reinforcement in those three specimens was gvien referring to the joint strength equations proposed in Japan.

However, it is insufficient to the requirements for the column-bars confinement in ACI 318-83 and also to the requirements for shear resistance in NZS 3101-1982. The specimen 'X2-3' was gvien a considerable amount of joint reinforcement of high strength steel according to the requirements of ACI Code or NZ Standard. The specimen 'X2-4' had an oblong joint resulting from deep beams : ($h_b/h_c=2$). The arrangement of the joint reinforcement was similar to X2-1. The specimens 'X2-1' and 'X2-4' were loaded laterally at the top of column in two beam-directions perpendicular to each other by changing the direction alternately at every cycle of loading. The specimens 'X2-2' and 'X2-3' were loaded in the same loading history to 'X2-1' except that loading directions were ± 45 degree in the beam-directions.

2.2 Properties of Materials

The mechanical properties of concrete and steel are shown in Table 2. Concrete was cast in an upright position of the subassemblage specimens by dividing into two stages at the top surface of the slab. Compressive strength of the concrete was 210 to 238 kgf/cm^2. The longitudinal bars in columns and beams were deformed bars of SD35 ($f_y=35$ kgf/mm^2). The transverse bars were round bars corresponding to SR30 ($f_y=30$ kgf/mm^2) except that high strength steel of 136 kgf/mm^2 in equivalent yield strength for 0.2% residual strain was used in the joint of X2-3.

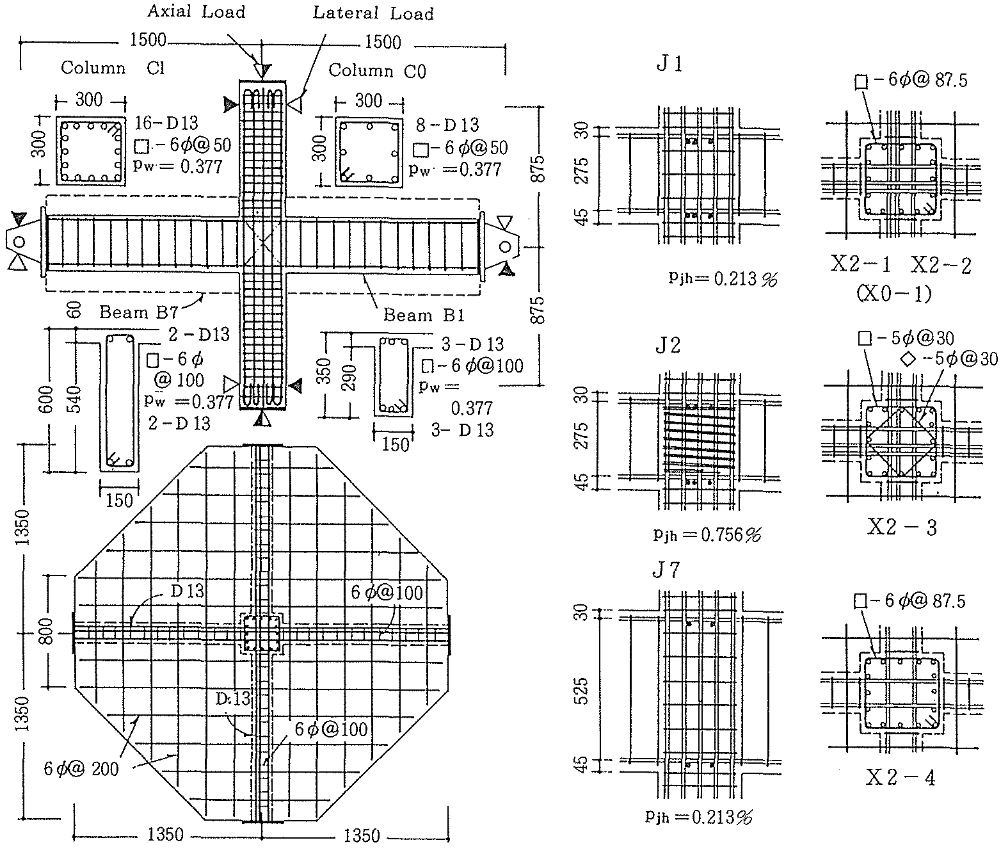

Fig. 1 Details of Specimens

Table 1 Properties of Specimens

Specimen	Type of frame	Type of members				Loading condition	
		Beam	Column	Joint	Slab	Lateral load	Vertical load
X2−1	two−way	B1	C1	J1	exist.	X and Y	Column axial
X2−2	two−way	B1	C1	J1	exist.	+45°and -45°	load stress
X2−3	two−way	B1	C1	J2	exist.	+45°and -45°	is 35kgf/cm²
X2−4	two−way	B7	C1	J7	exist.	X and Y	in all
X0−1	one−way	B1	C0	J1	non	X	specimens

Table 2 Properties of Materials

(a) Concrete (∗kgf/cm²)

Specimen	Secant modulus at $\sigma_{CB/3}$ ($\times 10^5$∗)	Compress. strength σ_{CB}(∗)	Strain at σ_{CB}(%)
X2−1	1.81	229	0.25
X2−2	1.80	227	0.25
X2−3	1.46	210	0.29
X2−4	1.67	238	0.27
X0−1	2.05	217	0.20

(b) Reinforcement (∗kgf/mm²)

Bar size	Yield stress(∗)	Fracture (∗)	Elongation (%)
D13	37.0	55.3	24.9
6φ 1)	33.9	42.8	23.0
6φ 2)	34.5	42.2	20.2
5φ	136.0	143.4	5.6

Note : 1) Shear reinforcement
2) Slab reinforcement

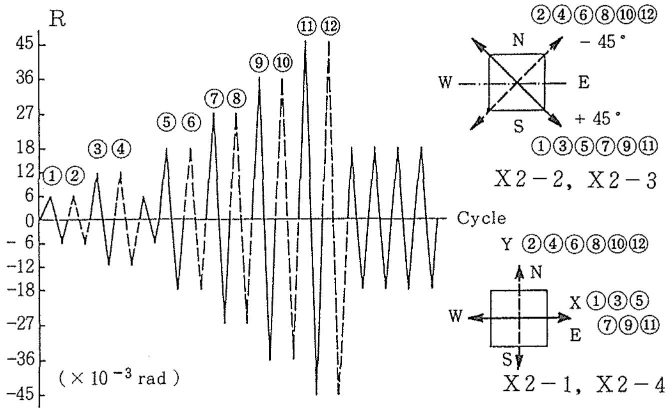

Fig. 2 Forced Displacement History

2.3 Instrumentation and Loading

The bottom of the column was supported by two lateral pins crossing at right angles and restricted against the horizontal displacement in any direction, while the beam ends were supported on vertical rigid members equipped with universal joints at both ends so as to be free to slide in any horizontal direction. Reversing horizontal bi-directional loads were applied at the top of the column with two actuators installed perpendicular to each other. The controlling history for story displacement was programmed as shown in Fig. 2. The axial column loading was applied with a hydraulic jack through an independent set of yokes and held constant at 35kgf/cm^2 during the tests.

3. Test Results and Discussion

3.1 Crack Patterns and Modes of Failure

The crack patterns on slabs of X2-1 after the test are shown in Fig. 3(a). In all specimens, while cracks caused by bending of the slab planes developed from the column faces toward the free ends of beams along the beam sides, another type of cracks penetrating the slab thickness appeared at an angle of about 45 degrees to the beam axes.

Occurrence of shear cracks on the faces of the joints, shown in Fig. 3, were completely not observed because of the existence of the transverse beams. However, it could be ascertained dy the abrupt increase of strains in the joint reinforcement. The values of the load and story drift angle at the first joint shear cracking obtained from the strain data are shown in Table 3.

At the stage of failure, crushing of concrete in the yield hinge region of beams was accompanied by crushing in the compressive zones of joints adjoining the beam ends. Spalling of shell concrete at the corners of joints was also observed.

3.2 Strength

Tables 3 and 4 show the summary of the test results and the comparison with the calculated values. The observed horizontal shear forces in the joints were estimated using

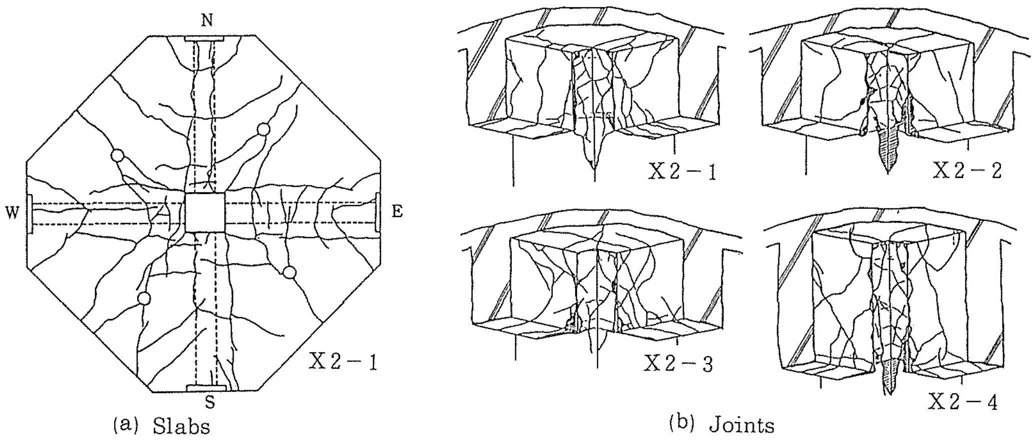

Fig. 3 Crack Patterns of Slabs and Joints after Tests

the following equation :

$$V_{jh}=(M_{b1}+M_{b2})/j_b-V_c \qquad (1)$$

(1) The effective width of slab

The yield moment in beam is defined here as the moment when the strain in the beam longitudinal reinforcement reaehes first the yield strain.

The column shear forces converted from the yield moments in beams of each specimen are shown in Table 3. Some examples of the strain distributions of slab reinforcement at the peaks of several loading cycles in X2-1 and X2-3 are shown in Fig. 4. Since the observed points in the slabs were located along the east side face of the south beam and the west side face of the north beam as shown in the figure, the strain distributions along both beams were in reverse conditions with each other, positive and negative, for the beam bending moments.

It should be noted that no compressive strain was observed at any points along the beams under any condition of beam moment from the early stages of loading cycles, except that very small compressive strain appeared at a few points during the first cycle in each specimen. In X2-1 loaded in the beam directions, the yielding of slab reinforcement initiated from the column sides at the peak of the third cycle in which the beam bar yielded, and the yield regions extended to the free ends of the beams at the seventh cycle in which the specimen exhibited the ultimate strength. The strains of X2-3 loaded in $\pm 45^\circ$ directions were smaller at parts adjoining the column and greater at parts around the free ends of beams than the strains at such parts of X2-1. In any specimen, it should be noted that strains of any slab reinforcement were in tension at the ultimate stage.

The values denoted as ${}_cV_{cy1}$, were estimated under the assumption that the yield stress of slab reinforcement arranged within the effective width equal to one-tenth of the span length on each side of beams participated in the bending strength of the beams. These values seem to be conservative in estimating the yield strength of frames in general. The values denoted as ${}_cV_{cy2}$ were calculated by using the effective width equal to one-fifth of the

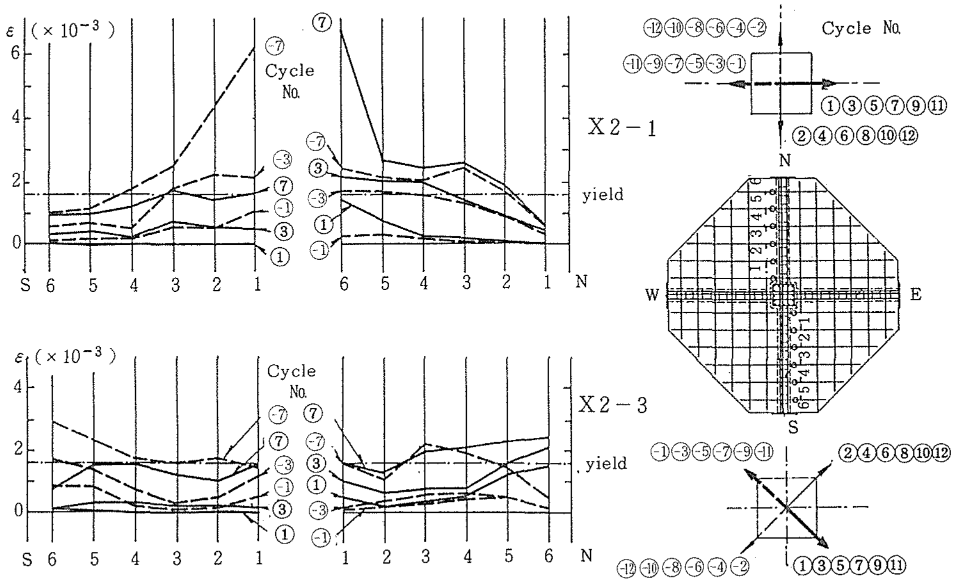

Fig. 4 Strain Distribution of Slab Reinforcement

span length, consequently these values seem to be adequate for X2-1 and X2-4, and to be excessive for X2-2 and X2-3.

(2) Ultimate strength

After the yielding of the beams, the lateral reinforcement in the joints began yielding except for the specimen 'X2-3'. The column shear forces and the joint shear forces at the ultimate strength of each specimen are shown in Table 4.

The specimen 'X2-3' attained the ultimate state without yielding of the lateral joint reinforcement. The test values of the ultimate joint shear force are compared with the values calculated using the empirical equations proposed by Kamimura (Eq. 2) and Koreishi (Eq. 3), and the values specified according to ACI 318-83 Appendix A and NZS 3101-1982 in Table 4.

$$v_{jh}=V_{jh}/b_j j_c=(0.78-0.0016f'_c)f'_c+0.5p_w f_y \quad [\text{kgf/cm}^2] \tag{2}$$

$$v_{jh}=V_{jh}/b_j j_c=(0.5-0.001f'_c)f'_c+2.7\sqrt{p_w f_y} \quad [\text{kgf/cm}^2] \tag{3}$$

where $b_j=(b_c+b_b)/2,\ j_c=7d_c/8$

As for the specimens loaded in 45° directions, X2-2 and X2-3, the assumption that the normalized interaction curve for bi-directional shear strength is expressed with an arc of a circle was adopted in the calculation using the equations (2), (3) and ACI. In the calculation according to NZS, it is permitted to consider that the joint shear strength would be fully effective separately in each of the two principal directions and then the resultant of the two-directional resistances is $\sqrt{2}$ times the uniaxial strength in these cases, while the contribution of concrete to the shear resistance must be reduced because of dividing the effect

Table 3 Test Results and Calculated Values

Specimen	Load direction		Panel initial shear cracking: Cycle	(1) $_tV_c$	(2) $_tR$	(3) $_tV_{jh}$	(4) $_cV_{jh}$	(5) (3)/(4)	Yelding in beams: Cycle	(6) $_tV_c$	(7) $_tR$	(8) $_cV_{cy1}$	(9) $_cV_{cy2}$	(10) (6)/(8)	(11) (6)/(9)
X2-1	X	+	3	6.33	6.87	36.1	34.7	1.05	3	7.15	8.32	5.40	6.08	1.32	1.18
		−	3	6.00	6.10	34.2		0.99	3	6.49	7.49			1.20	1.07
	Y	+	2	5.64	4.89	31.8		0.92	2	5.64	4.89	5.33	6.02	1.06	0.93
		−	2	5.21	4.69	29.6		0.86	4	5.40	6.66			1.01	0.89
X2-2	+45°	+	3	6.91	7.37	39.4	34.4	1.15	3	7.43	8.58	7.59	8.55	0.98	0.87
		−	3	7.65	9.21	43.6		1.27	3	7.65	9.17			1.01	0.89
X2-3	+45°	+	3	5.74	5.88	32.7	33.5	0.98	3	8.06	9.25	7.59	8.55	1.06	0.94
		−	3	5.88	6.10	33.4		0.99	3	6.80	7.36			0.90	0.80
X2-4	X	+	3	9.45	14.87	24.1	35.0	0.69	1	9.95	4.65	6.68	7.05	1.49	1.41
		−	7	11.15	9.43	28.5		0.81	1	8.50	2.03			1.27	1.21
	Y	+	4	9.26	6.72	23.5		0.67	2	9.05	4.36	6.68	7.16	1.35	1.26
		−	4	9.73	8.69	24.6		0.72	2	9.05	4.36			1.35	1.26

$_cV$, $_cv$: Calculated value
$_tV$, $_tv$, $_tR$: Test value
V_c : Shearforce of column [tonf]
V_{jh} : Shearforce of joint [tonf]
v_{jh} : Shear stress of joint [kgf/cm²]
R : Story drift angle [$\times 10^{-3}$ rad]

$$_cV_{cy} = \{(M_{by} + M'_{by}) / (\ell_b - D_c)\} \cdot \ell_b / \ell_c$$

where, $M_{by} = 0.9 \cdot {}_ba_t \cdot {}_b\sigma_y \cdot d$,
$M'_{by} = 0.9({}_ba_t \cdot {}_b\sigma_y + {}_sa_t \cdot {}_s\sigma_y) \cdot d$

$_cV_{cy1}$, and $_cV_{cy2}$: calculated from M'_{by} including slab bars within effective width of $0.1\ell_b$ and $0.2\ell_b$, respectively, where ℓ_b=span length of beam, ℓ_c=story hight.

$$_cV_{jh} = \frac{1}{b_j \cdot j_b \cdot j_c}(M_b + M'_b - V_c \cdot j_b)$$

where, $j = \frac{7}{8}d$, b_j=column width

Table 4 Test Results and Calculated Values at Ultimate Stage

(units : V=tonf, R=10^{-3} rad.)

Specimen				X2−1	X2−2	X2−3[5]	X2−4	X0−1
Observed	X or +45°	+	$_tV_c$	7.9	9.7	10.3	11.5	6.2
			$_tR$	25.9	17.4	27.5	26.9	32.3
			$_tV_{jh}$	36.7	44.7	47.4	24.7	29.4
		−	$_tV_c$	7.6	9.4	9.8	11.4	5.8
			$_tR$	19.1	27.5	36.3	29.5	32.3
			$_tV_{jh}$	36.3	43.2	45.5	24.6	27.0
Design[1]	$_DV_{jh}$[2]			24.8	35.1	35.1	14.0	25.3
	($_DV_{jh}'$)[3]			(32.6)	(46.0)	(46.0)	(20.5)	−
Calculated	Kamimura		V_{ch}	50.3	50.2	49.5	50.4	48.9
			V_{sh}	1.9	1.9	8.1	1.9	1.8
			V_{jh}	52.2	52.1	57.6	52.3	50.7
	Koreishi		V_{ch}	32.8	32.8	32.8	33.1	32.6
			V_{sh}	3.9	3.9	7.9	3.9	3.7
			V_{jh}	36.7	36.7	32.8	37.0	36.3
	ACI[4]		V_{jh}	46.1	45.9	44.2	47.0	33.8
	NZS-3101		V_{ch}	6.6	0	0	6.3	6.9
			V_{sh}	5.7	8.1	34.8	11.5	5.3
			V_{jh}	12.3	8.1	34.8	17.8	12.2

V_{ch}, V_{sh} : Joint shear strength provided by concrete resisting mechanism and by horizontal joint reinforcement, respectively

1) Joint shear strength required beam yielding
2) estimated with slab effective width=$b_w + 0.2\ell_b$
3) estimated with entire slab width
4) Code of ACI 318−1983, $V_{jh} = V_{ch}$
5) calculated with observed joint reinforcement stress of f_y=4.08 tonf/cm²

of column compression according to the equation :

$$V_{ch}/b_j h_c = 2C_j P_e/3A_g - f'_c/10 \quad [\mathrm{MPa}] \tag{4}$$

where $C_j = V_{jh}/(V_{jx} + V_{jy})$

In the case of the present specimens $C_j = 1/2$ and $C_j P_e/A_g < f'_c/10$. The following behavior could be derived from the Table ; (i) some enhancement of strength was brought out in the space frames in comparison with the one-way frame ; (ii) the bi-directional shear strength of space frames which resulted from the bending strengths of beams and slabs was higher than the principal directional shear strength, though less than $\sqrt{2}$ times ; (iii) heavy reinforcement of high strength steel was not so effective as it would be expected from the equations. It might be considered that the strength enhancement in X2-1 would be caused by the participation of the slabs in raising the yield strength of beams and in delaying the slippage of beam bars from the joint, and by the participation of the transverse beams in keeping the joint shear stiffness.

3.3 Relationship between Load and Deformation

Lateral shear force - story drift angle relation curves are shown in Fig. 5, where the lateral shear force 'V' and the story drift angle 'R' are presented with a suffix letter expressing their vector components in X or Y direction for the specimens X2-1 and X2-4, or in $+45°$ or $-45°$ direction for X2-2 and X2-3. The strength decline after the ultimate strength was the severest in the specimen X2-4 with the oblong joint panel, and was the slightest in the specimen X2-3 with the high lateral joint reinforcement. The shapes of V-R loop at X-directional loading and Y-directional loading were similar to each other, but those at $-45°$ directional loading were slenderer than those at $+45°$ directional loading. The joint shear deformation of X2-3 was slightly small against the other specimens, but increased gradually with the progress of loading cycles without yielding of the joint reinforcement.

3.4 Components of Story Drift Caused by Local Deformations

Fig. 6 shows the relations between the story drift angle 'R' and the consisting ratios of the components of the story drift 'δ' or of the energy absorption 'W'. The variables 'δ' and 'W' caused by the joint panel shear deformation are signified with 'P', and those caused by the beam rotation at the adjoining end are signified with 'B' in every specimen.

The vertical axes of the figure express the proportion of the component of 'δ' or 'W' against the whole value, or express the constituent values of 'W' in X or Y direction of X2-1 and X2-4 and in $+45°$ or $-45°$ direction of X2-2 and X2-3. The horizontal axes express the story drift angle in each direction. The beam rotation was evaluated by using couples of relative displacements between the column face and the measuring points set on the top and bottom faces of beam ends.

The proportions of story drifts caused by the beam end rotations to the whole story drifts in each specimen were almost same between the X and Y or $+45°$ and $-45°$ directions. The proportions of story drifts caused by the joint panel shear deformations in direction Y or $-45°$ were larger than those in direction X or $+45°$, respectively, except for the specimen

X2-3.

Energy absorption, W_T, W_P and W_B, were obtained in each cycle of load reversals from loop areas in the relation curves of the shear force and the whole story drift or the component. The whole energy absorption 'W_T' increased after yielding of beam bars in every specimens. W_T at the Y-directional loading of X2-1 or X2-4 became less than W_T at X-directional loading after ultimate strength, that above 15×10^{-3} radian in story drift angle.

The inferiority of W_T at $-45°$ directional loading to W_T at $+45°$ directional loading of X2-2 or X2-3 appeared even in a small range of story drift, because in the north-south beam, duplication of half cyclic loadings in the same sign range were repeated alternately in north and south directions as shown in Fig. 7. As compared with X2-1, W_T of X2-2 was slightly smaller in any story drift level due to bi-directional loading, but the capacity for energy absorption could be improved by arrangement of high lateral joint reinforcement especially at the ultimate stage.

V; [tonf], R; [10^{-3} rad.], ▲ ;Yield Strength, △ ;Ultimate Strenghth

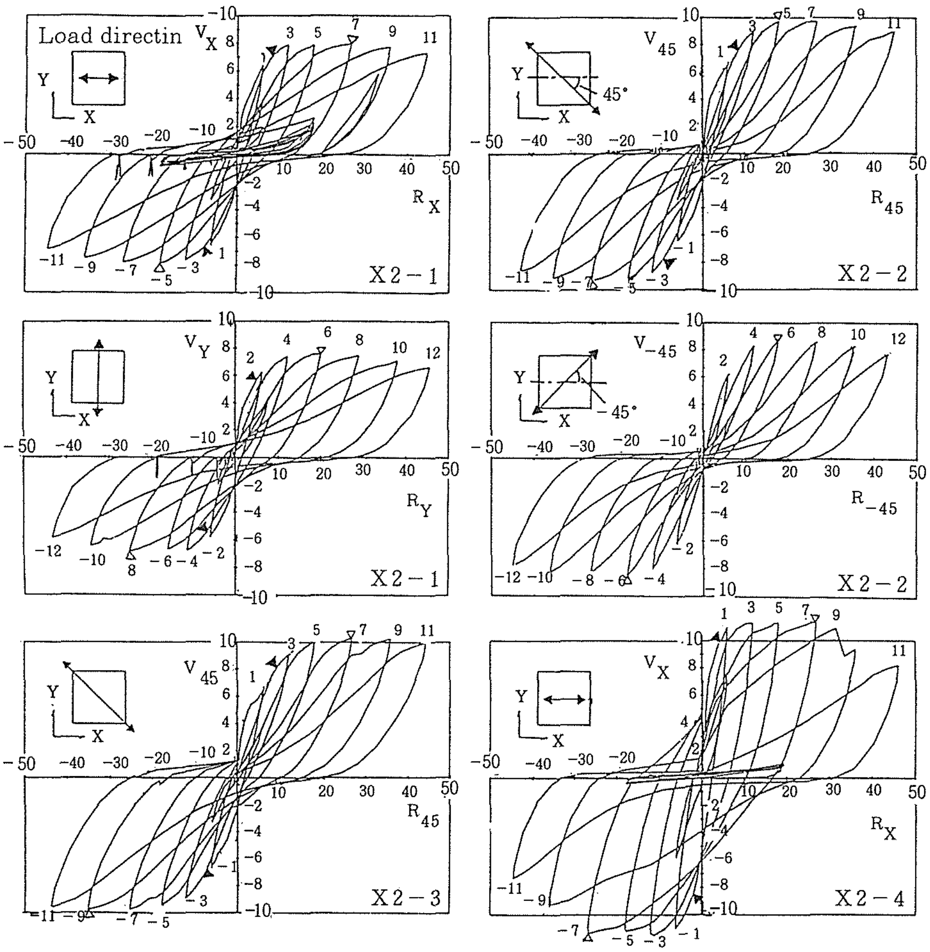

Fig. 5 Lateral Shear Force－Story Drift Angle Relation Curves

The energy absorption in joint panel 'W_P' were almost the same in any specimen and in any directional loading, except that W_P in Y-directional loading were larger than W_P in X-directional loading.

3.5 Characteristics of Lateral Joint Reinforcement

The hoops in the joints of X2-1, X2-2 and X2-4, provided with ordinary steel bars and with low reinforcement bar ratio of 0.213%, yielded at the strain of 0.18% after the beam bar yielding and before the ultimate strength of space frames. The hoops and diamond ties in the joint of X2-3, provided with high strength steel bars and with high reinforcement bar ratio of 0.756%, reached about 0.25% in maximum strain without yielding. These behaviors can be seen in Fig. 8. The strains of every hoop in beam-directional loading specimens exhibited different values between the legs arranged in parallel with and in perpendicular to the loading

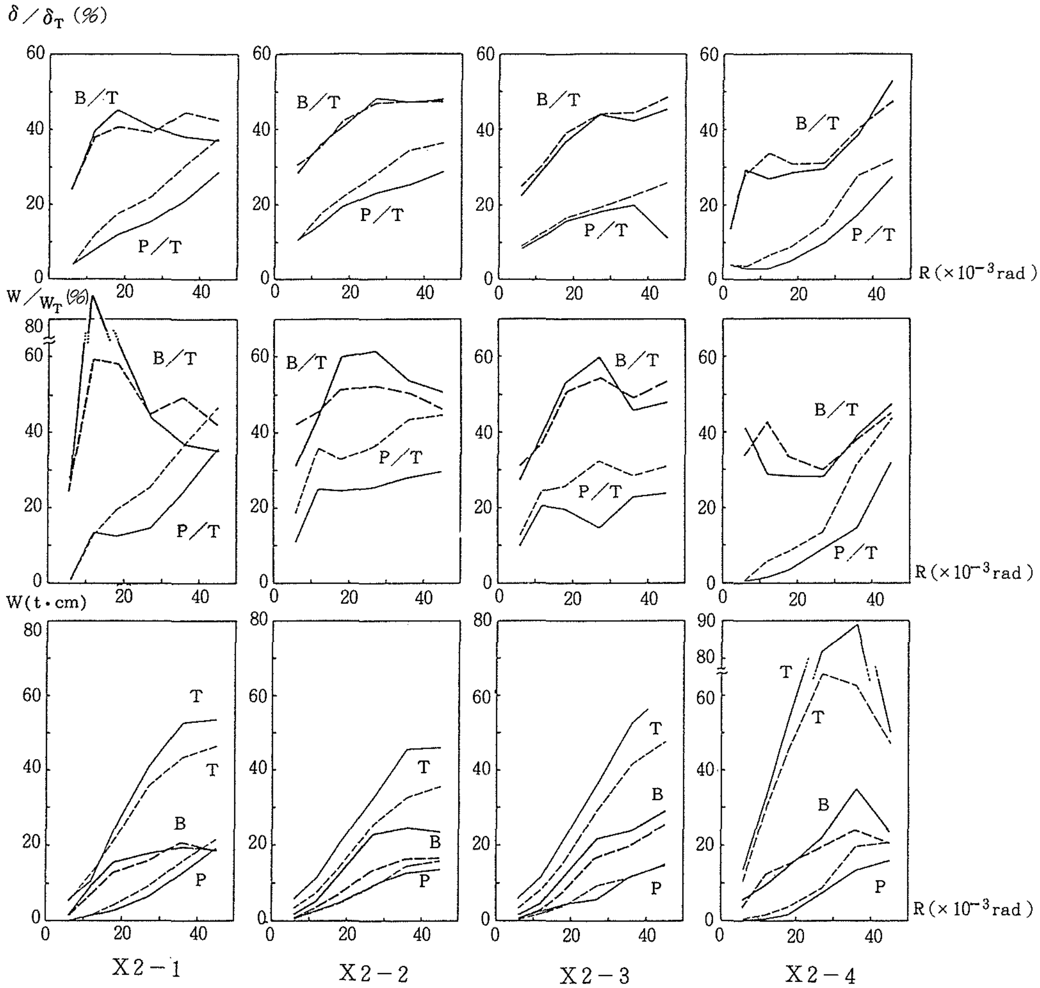

Note : T=the Whole Values, P=Constitutive Values Caused by Joints Panel Shear Deformation, B=Constitutive Values caused by Beam End Rotation, R= Story Drift Angle
——— at Loading in X or +45°Direction, – – – at Loading in Y or −45° Direction

Fig. 6 Constitutive Values of Story Drift "δ" and Energy Absorption "W" direction, because the parallel legs mainly resisted the shear force in the joint and the perpendicular legs worked as the confinement against the compression force. The strain value of the former was from 1.5 to 2 times larger than that of the latter.

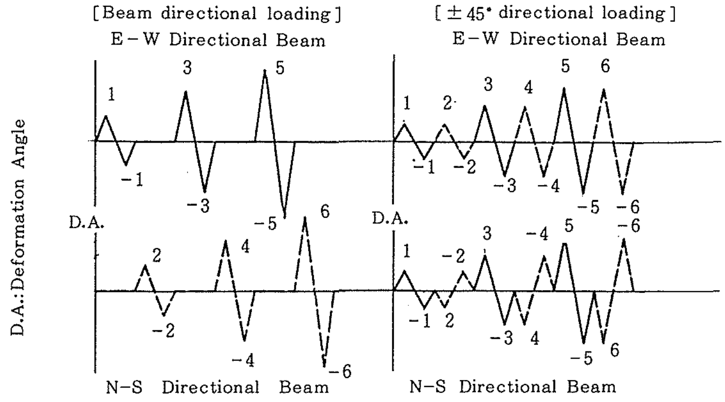

Fig. 7 Loading History of Each Beam

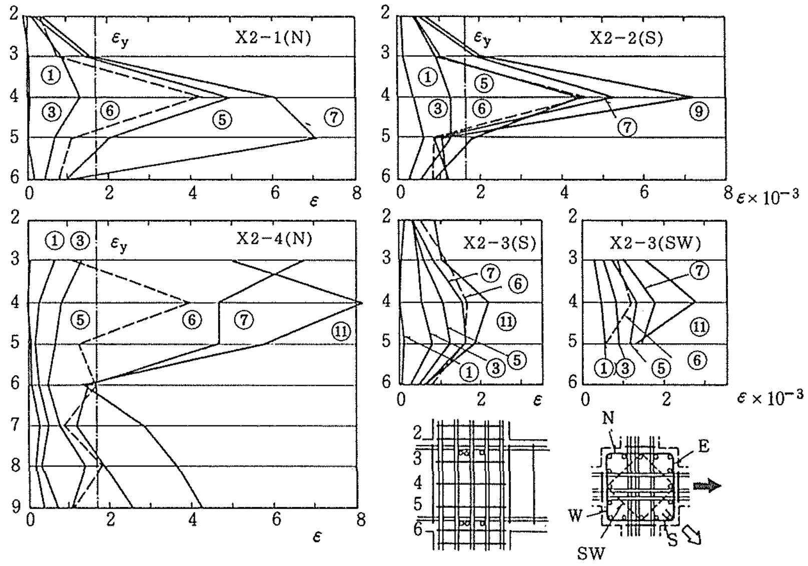

Fig. 8 Strain Distribution of Joint Hoops

4. Conclusions

(1) Shear cracking stress in the beam-column joint could be assessed with the principal stress concept by assuming the normalized interaction curve of an arc of circle for the bi-directional shear, but some modification should be necessary for the shear cracking stress decline in oblong joints.

(2) The effective width of slab to participate in the bending resistance of beam will be taken

as about one-tenth of span length for the conservative purpose and about one-fifth of span length at the yielding of beams. For the estimation of design shear forces in the joint, the effective width should be taken as the entire width of slab. The effective width of slab subjected to bi-directional loading is smaller than that mentioned above.

(3) The enhancement of joint shear strength by the transverse beams which have yield hinges at the column faces should not be expected for cracking strength.

(4) Calculated values of shear strength of joint panels using the two equations proposed in Japan or according to the requirements of ACI Code or NZS did not show good agreement with the observed values. Further investigation should be necessary.

(5) The yielding of beams prior to injury in joints by shear should not always assure the ductile behavior of frames. The ultimate shear strength or shear stiffness of joint panel after yielding of adjacent beams or columns should be dependent to the intended limit of story drift of frames.

(6) The slippage of top beam bars pulling out from the joint panel was smaller than that of bottom beam bars due to restraint of the slab. In the frames subjected to bi-directional loading, the slippage of beam bars was a somewhat larger as compared with that in the frames subjected to beam directional loading.

(7) The capacity of energy absorption in space frames did not show a remarkable difference for any lateral loading directions. However, the amounts of energy absorption varied with different loading histories.

Acknowledgment

The authors are deeply grateful to Associate Professor T. Kusakari of Kushiro Technical College, Hokkaido, for his assistance in the experimental work in this paper when he was a graduate student.

References

1. Suzuki, N., Otani, S. and Kobayashi, Y. : Proc. 8th WCEE, (1984), Vol.6, p.453
2. Chen, Y., Chen, G. and Gao, H. : Report of U.S.-N.Z.-Japan-China Seminar on the Design of R/C Beam-Column Joints for Earthquake Resistance, (1987), 15, p.1
3. Fujii, S. and Morita, S. : Report of U.S.-N.Z.-Japan-China Seminar on the Design of R/C Beam-Column Joints for Earthquake Resistance, (1987), 13, p.1
4. Kamimura, T : Proc. A.I.J. Annual meeting, (1971), p.1155 (in Japanese)
5. Koreishi, : Master thesis of University of Tokyo, (1971), p.1(in Japanese)
6. American Concrete Institute : Building Code Requirements for Reinforced Concrete (ACI 318M-83), (1984), p.88
7. Standard Association of New Zealand : Code of Practice for The Design of Concrete Structures (NZS 3101), (1982), p.1